Arabian Journal for Science and Engineering (2021) 46:6049–6059
https://doi.org/10.1007/s13369-020-05297-6

RESEARCH ARTICLE-PHYSICS

# Numerical Study of Nanofluid Transport Subjected to the Collective Approach of Generalized Slip Condition and Radiative Phenomenon

S. Z. Abbas[1,6] · S. Farooq[2] · Y. M. Chu[3,4] · W. Chammam[5] · W. A. Khan[6] · A. Riahi[5] · H. A. Rebei[7] · M. Zaway[8]

Received: 12 March 2020 / Accepted: 30 December 2020 / Published online: 28 January 2021


**Abstract**
This study investigates theoretically, the effects of axisymmetric magnetohydrodynamic stagnation point flow of nanofluid over a surface lubricated by taking the general slip condition: The application perspective in biological farming and irrigation system. The impacts of radiation, chemical reaction, thermophoresis, and Brownian motions are further taken into account. In this model, PDEs are appropriately transformed into dimensionless ODEs. A numeric techniques BVP4C is implemented for the solutions of all the involved transport variables. Influences by the physical significance parameters on the velocity, temperature, and concentration profiles are studied. Physically, the effects of the skin friction coefficient on the heat transfer and concentration rate at the surface are analyzed. The Lorentz force has visible diversity on the flow properties. A transition of slip to no-slip condition is evident in the present study.

**Keywords** Radiative heat flux · Chemical reaction · Thermophoresis and Brownian motions · Generalized slip constraints · BVP4C

## 1 Introduction

In the progress of nanotechnology, a crucial role is played by transportation phenomena. In biological farming, we often come across the flow of fluids over the lubricated surface. To advance the transfer of energies between the source and consumer, the researchers are on the way toward the optimistic methods. Specifically, it is perceived that heat transmission could be made more efficient by adding extra small matter particles in the liquids. In Scientific language, these particles are famous as nanoparticles, and the liquid prior to the mixture is base liquid. Such a combination is named the nanofluids. The base liquid's nature determines the flow properties' responses and the type of particles added. The preparation of these liquids is carried out in two different procedures. In the first one, known as the two-step method, the prepared nanoparticles are hanged in the base liquids, while in the second one, the same particles are dispersed in the base liquids. The fundamental concern is the stability and the homogeneity, which are always taken in these methods to prepare nanoliquids. Specifically, erosion, obstruction, and clustering need to be taken into account. As the cooling and heating agents, the nanoliquids have shown the best performance until now.

✉ Y. M. Chu
chuyuming@zjhu.edu.cn

✉ W. Chammam
w.chammam@mu.edu.sa

[1] Department of Mathematics and Statistics, Hazara University Mansehra, Dhodial, Pakistan

[2] Department of Mathematics and Statistics, Riphah International University, Islamabad 44000, Pakistan

[3] Department of Mathematics, Huzhou University, Huzhou 313000, People's Republic of China

[4] Hunan Provincial Key Laboratory of Mathematical Modeling and Analysis in Engineering, Changsha University of Science and Technology, Changsha 410114, People's Republic of China

[5] Department of Mathematics, College of Science Al-Zulfi, Majmaah University, P.O. Box 66, Al-Majmaah 11952, Saudi Arabia

[6] School of Mathematics and Statistics, Beijing Institute of Technology, Beijing, China

[7] Department of Mathematics, College of Science, Qassim University, Buraydah, Saudi Arabia

[8] Department of Mathematics, College of Science and Humanities, AdDwadimi, Shaqra University, Shaqraa, Saudi Arabia

The idea of nanoliqiuds was initiated by Choi et al. [1], which was tested as the source of heat transfer. The thought brought into several kinds of research of fluids mechanics. For the convected flow of heat, Oztop, and Abu-Nada [2] investigated the Oldroyd-B model. The same model is studied by Khan et al. [3] for 3D flow using the heat sink-source phenomena. The MHD effects are investigated by Sheikholeslami et al. [4]. The peristalsis flow of nanofluid with MHD-indeed studied by Akbar et al. [5]. Several investigations are carried out for non-Newtonian fluids, Sandeep et al. [6] checked the non-Newtonian fluids with nanoparticles. Further, the entropy generation is studied in [7] by Rehman et al.

The study of nanofluids with a specific choice of base liquid and nanoparticles is carried as well. As a base liquid considering $H_2O$ and $C_2H_6O_2$, with the nanoparticles as Cu, the study is contributed by Haq et al. [8] by taken two parallel disks. Considering the impact of slip on non-Newtonian fluid with nanoparticles is investigated by Rahman et al. [9] for tapered artery stenosis. The chemical processes have a visible effect on the flow phenomena. Considering the rotating disk, the impact of chemical processes is studied by Hayat et al. [10]. The same is studied for MHD effects by Hayat et al. [11]. With the consideration of thin film, the study of MHD flow is contributed by Sandeep [12].

In the general view of chemical reactions, we have two procedures. The first one takes a Stoichiometric and rate equation pair, while the other could have multi Stoichiometric equations only.

For a variety of responses, the chemical reactions are termed as homogeneous and heterogeneous, occurrence in single-phase and multi-phase, respectively.

The chemical reactions have a significant role in the fluid flows. The first modeling of Activation energy and chemical reaction initially formulated by Ramzan et al. [13] considering magneto-nanofluid. On the same model, the radiative flow is contributed by Ramzan et al. [14] with double stratification of Powell-Eyring. In rotating disk flow of Maxwell fluid with activation energy explored by Shafique et al. [15]. Khan et al. [16, 17] extended it to 3D flow for higher models, including Burgers and generalized. The effects of MHD are studied by Mustafa et al. [18], utilizing chemical reaction and activation energy. The nanofluid study is dedicated to a variety of scenarios in [19–24]. The technique BVP4C is applied to several studies for the numerical solution of differential equations [25–36].

In this theoretical work, given the above studies, we extracted the features of stagnation point flow for 2D steady axisymmetric nanofluid pointing lubricated plate with radiation and chemical reaction considering the generalized slip condition, which has not been presented by any literature before. Via appropriate transformations, we converted the PDEs system to dimensionless ODEs using nonlinear slip conditions at the boundary. For the required solution, we used the BVP4C, a built-in MATLAB technique, to find the solutions of the governing equations. A comparison of the skin friction with the studies [37, 38] is also conducted.

## 2 Modeling

To develop the mathematical model, we consider the lubricated surface such that the flow is steady and axisymmetric, having a stagnation point for an incompressible fluid. Further, the small Reynolds number is taken for the effects of magnetic force. The flow analysis is executed in a chemical reaction and radiation environment with the effects of thermophoresis and Brownian motions. A pseudo-geometry is displayed through Fig. 1.

The axisymmetry demolished the azimuthal component, so the component of velocity for the fluid and lubrication is taken as $[u1(r,z),0,u3(r,z)]$ and $[U1(r,z),0,U3(r,z)]$, respectively. For the mathematical simplification, we assume the sheet is showered with power-law lubrication, creating a thin layer with varying thickness $h(r)$. The flow rate $Q$ is given as

$$Q = \int_0^{h(r)} 2\pi r U1 \mathrm{d}z \tag{1}$$

The fundamental governing PDEs are as below

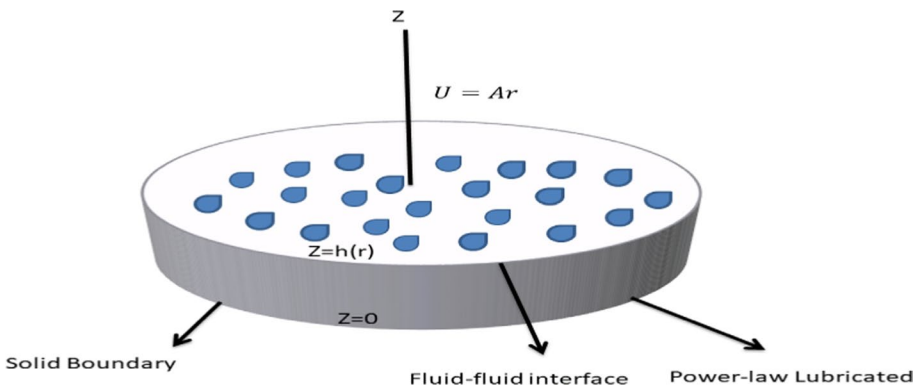


**Fig. 1** Geometry of the model

$$\frac{\partial u1}{\partial r} + \frac{u1}{r} + \frac{\partial u3}{\partial z} = 0, \tag{2}$$

$$u1\frac{\partial u1}{\partial r} + u3\frac{\partial u1}{\partial z} = -\frac{1}{\rho}\frac{\partial p}{\partial r} + \nu\left\{\frac{\partial^2 u1}{\partial r^2} + \frac{\partial}{\partial r}\left(\frac{u1}{r}\right) + \frac{\partial^2 u1}{\partial z^2}\right\} - \frac{\sigma B_0^2 u1}{\rho}, \tag{3}$$

$$u1\frac{\partial u3}{\partial r} + u3\frac{\partial u3}{\partial z} = -\frac{1}{\rho}\frac{\partial p}{\partial z} + \nu\left\{\frac{\partial^2 u3}{\partial r^2} + \frac{\partial^2 u3}{\partial z^2} + \frac{1}{r}\frac{\partial u3}{\partial r}\right\}, \tag{4}$$

$$u1\frac{\partial T}{\partial r} + u3\frac{\partial T}{\partial z} = \alpha\left(\frac{1}{r}\frac{\partial T}{\partial z} + \frac{\partial^2 T}{\partial z^2}\right) + \tau\left(D_{\mathrm{B}}\frac{\partial T}{\partial z}\frac{\partial C}{\partial z} + \frac{DT}{T\infty}\left(\frac{\partial T}{\partial z}\right)^2\right) - \frac{1}{\rho C_p}\frac{\partial q_r}{\partial z}, \tag{5}$$

$$u1\frac{\partial C}{\partial r} + u3\frac{\partial C}{\partial z} = D_{\mathrm{B}}\left(\frac{1}{r}\frac{\partial C}{\partial z} + \frac{\partial^2 C}{\partial z^2}\right) + \frac{DT}{T\infty}\left(\left(\frac{1}{r}\frac{\partial T}{\partial z} + \frac{\partial^2 T}{\partial z^2}\right)\right) - k_1(C - C_\infty), \tag{6}$$

where the involved quantities are defined in the nomenclature below:

| Nomenclature | |
|---|---|
| $u1$ | Velocity component along $r$-axis |
| $u3$ | Velocity along $z$-axis |
| $p$ | Pressure |
| $\alpha$ | Material parameter |
| $\nu$ | Kinematic viscosity |
| $T$ | Temperature |
| $T_\infty$ | Ambient temperature |
| $D_{\mathrm{B}}$ | Thermophoresis parameter |
| $D_{\mathrm{T}}$ | Brownian motion parameter |
| $C$ | The concentration of the fluid |
| $k_1$ | Chemical reaction |
| $\sigma$ | Electrical conductivity |

From [10] for the Roseland approximation, the radioactive heat flux term is

$$q_{\mathrm{r}} = -\frac{4\sigma^*}{3k^*}\frac{\partial T^4}{\partial z}, \tag{7}$$

where $k^*$ is the mean absorption coefficient and $\sigma^*$ is Stefan Boltzmann constant. We can assume the temperature difference within the flow as a linear combination of temperature $T^4$ omitting the term with higher-order using Taylor's expansion we get

$$T^4 = 4TT_\nu^3 - 3T_\infty^4. \tag{8}$$

Then we have

$$\frac{\partial q_{\mathrm{r}}}{\partial z} = \frac{-16T_\nu^3\sigma^*}{3k^*}\frac{\partial^2 T}{\partial z^2}. \tag{9}$$

At the surface the no-slip boundary conditions have the form

$$U1 = 0 = U3, \quad T = T_w, \quad C = C_w \quad \text{at } z = 0, \tag{10}$$

and

$$U1 = 0 \quad \text{for } z \in [0,\ h(r)]. \tag{11}$$

the interfacial condition is [29]

$$u\frac{\partial u}{\partial z} = k\left(\frac{\partial U}{\partial z}\right)^n\left[1 - \beta^* k\left(\frac{\partial U}{\partial z}\right)^n\right]^{-\frac{1}{2}}. \tag{12}$$

Here $\beta^*$, $k$, and $n$ are the reciprocal of some critical shear rate, the consistency index, and the power-law index, respectively. Now use the following

$$U1(r,z) = \frac{\widehat{U}1(r)sz}{h(r)}. \tag{13}$$

Here $\widehat{U}1(r)$ is the component of velocity at the interfacial condition for both the fluids. The thickness is expressed as

$$h(r) = \frac{Q}{\pi r\widehat{U}1(r)}. \tag{14}$$

Substituting Eqs. 11 & 12 and $\widehat{U}1 \cong u$ into Eq. 10, we get

$$\frac{\partial u}{\partial z} = \frac{k}{\mu}\left(\frac{\pi}{Q}\right)^n r^n u^{2n}\left[1 - \beta^* k\left(\frac{\pi}{Q}\right)^n r^n u^{2n}\right]^{-\frac{1}{2}}. \tag{15}$$

Continuity of the velocities for fluid and lubricant at the interfacial condition given as

$$u3(r,h(r)) = U3(r,h(r)). \tag{16}$$

From Eq. 11 this further gives

$$u3(r,h(r)) = 0. \tag{17}$$

At the interfacial condition, the pressure distribution of pressure considered as

$$p(r,h(r)) = -\rho\frac{A^2r^2}{2}, \tag{18}$$

and

$$u1 = Ar, \quad u3 = -2Az, \quad T \to T_\infty, \quad C \to C_\infty, \quad \text{as } z \to \infty. \tag{19}$$

We take the dimensionless transformation of PDEs to ODEs as

$$\eta = z\sqrt{\frac{A}{\nu}},\ u1 = Arf'(\eta),\ u3 = -2\sqrt{A\nu}f(\eta),\ p = A\mu p^*(\eta) - \rho\frac{A^2r^2}{2},$$
$$\phi(\eta) = \frac{C - C_\infty}{C_w - C_\infty},\ \theta(\eta) = \frac{T - T_\infty}{T_w - T_\infty}. \tag{20}$$

Equation 2 is satisfied identically, and Eqs. 3, 4, 13, 15–19 become

$$f'''(\eta) - f'^2(\eta) + 2f(\eta)f''(\eta) + M\big(1 - f'(\eta)\big) + 1 = 0, \tag{21}$$

$$p^{*'}(\eta) = -2f''(\eta) - 4f(\eta)f'(\eta), \tag{22}$$

$$(1 + \mathrm{Rd})\theta''(\eta) + \mathrm{Pr}\big(2f(\eta)\theta'(\eta) + N_\mathrm{b}\phi'(\eta)\theta'(\eta) + N_\mathrm{t}\theta'^2(\eta)\big) = 0, \tag{23}$$

$$\phi''(\eta) + 2\mathrm{Le}f(\eta)\phi'(\eta) + \gamma\phi(\eta) + \frac{N_\mathrm{t}}{N_\mathrm{b}}\theta''(\eta) = 0. \tag{24}$$

The transformed boundary conditions are

$$f(0) = 0,\ f''(0) = \lambda\{f'(0)\}^n\left[1 - \beta f'(0)^n\right]^{-\frac{1}{2}},\ \theta(0) = 1,\ \phi(0) = 1,$$
$$p^*(0) = 0,\ f'(\infty) = 1,\ \theta(\infty) = 0,\ \phi(\infty) = 0. \tag{25}$$

In these equations, we take

$$M = \frac{\sigma B_0^2}{\sigma a},\ \mathrm{Pr} = \frac{\mu C_p}{\alpha},\ \gamma = \frac{C - C_\infty}{\alpha},$$
$$\lambda = \frac{k\sqrt{\nu}}{\mu}\left(\frac{\pi}{Q}\right)^{\frac{1}{3}}\frac{A^{\frac{2}{3}}}{A^{\frac{3}{2}}},\ \beta = \beta^* k\left(\frac{\pi}{Q}\right)^{\frac{1}{3}} rA^{\frac{2}{3}},$$
$$R_d = \frac{16T_\infty^3\sigma^*}{3k^*\alpha}, \mathrm{Nb} = \frac{\bar{C}\big(C_w - C\infty\big)}{\nu},$$
$$\mathrm{Nt} = \frac{D_\mathrm{T}\big(T_w - T\infty\big)}{T_\infty} \text{ and } \mathrm{Le} = \frac{\big(C_w - C\infty\big)}{D_\mathrm{B}}$$

are the magnetic parameter, Prandtl number, the reaction parameter, slip parameter, the generalized slip the radiation parameter, thermophoresis, Brownian motion parameter, and the Lewis number, respectively.

## 3 Solution Methodology

For the required information out of these equations, it is mandatory to find their solution. In our prosed model, the differential system is highly nonlinear, and it is not possible to find the exact solution. To deal with these equations, we utilized the MATLAB built-in technique BVP4C for these equations' numerical solution. This technique is based on the newton finite difference scheme. We used it to solve the Eqs. 21–24 by using boundary conditions in Eq. 25 for $f'(\eta)$, $f''(\eta)$, $\theta(\eta)$, $\phi(\eta)$, $\theta'(\eta)$, and $\phi'(\eta)$ for the designated values of involved parameters.

A general scheme of the methodology followed as:

Covert the higher-order ODEs in Eqs. 21–24 to the first order by setting

$$y1 = f,\ y2 = f',\ y3 = f'',\ yy1 = f''',\ y4 = \theta,\ y5 = \theta',$$
$$yy2 = \theta'',\ y6 = \phi,\ y7 = \phi',\ yy3 = \phi''$$

and solve Eqs. 21, 22, and 24 for $yy1$, $yy2$, and $yy3$, respectively. Then by embedding this scheme in BVP4C, we arrived at the outcomes in Figs. 2, 3, 4, 5, 6, and 7.

## 4 Discussion

The major outcomes are signified by sketching the numeric data through graphs and tables.

Here, in this section, we discussed the impact of involved parameters on the ultimate flow properties, the velocity profile $f'(\eta)$, temperature distribution $\theta(\eta)$, and the concentration $\phi(\eta)$ behavior is shown in Figs. 2, 3, 4, 5, 6, and 7.

### 4.1 Effects of slip Parameter $\lambda$

Specifically, Fig. 2a–c gives the act of slip parameter $\lambda$ on $f'(\eta)$, $\theta(\eta)$, and $\phi(\eta)$ the velocity, temperature, and concentration profile, respectively, for the fixed values of $\beta$, and $M$ as indicated in the figure. The cases $\lambda \to \infty$, and $\lambda \to 0$ interpreted as the no-slip and full slip conditions, respectively. The flowing fluid velocity increases for the no-slip state, while it is constant for the complete slip condition, see Fig. 2a.

Physically, we could establish that the higher rate of lubrication increases the velocity, and for the full slip, the fluid viscosity is crushed by the lubricant process. The influence on the temperature profile by the slip parameter $\lambda$ is shown in Fig. 2b. It is perceived that the temperature is enhancing by the growing values of the slip parameter.

Physically, the growing slip increases the flow velocity. As a result, the temperature at the wall is declined.

### 4.2 Effects of Generalized Slip Parameter $\beta$

A likewise behavior of concentration profile is recorded; see Fig. 3c. The growing slip parameter boosted the concentration. Through Fig. 3a–c, we sketched the effect of generalized slip parameter $\beta$ on the velocity, temperature, and

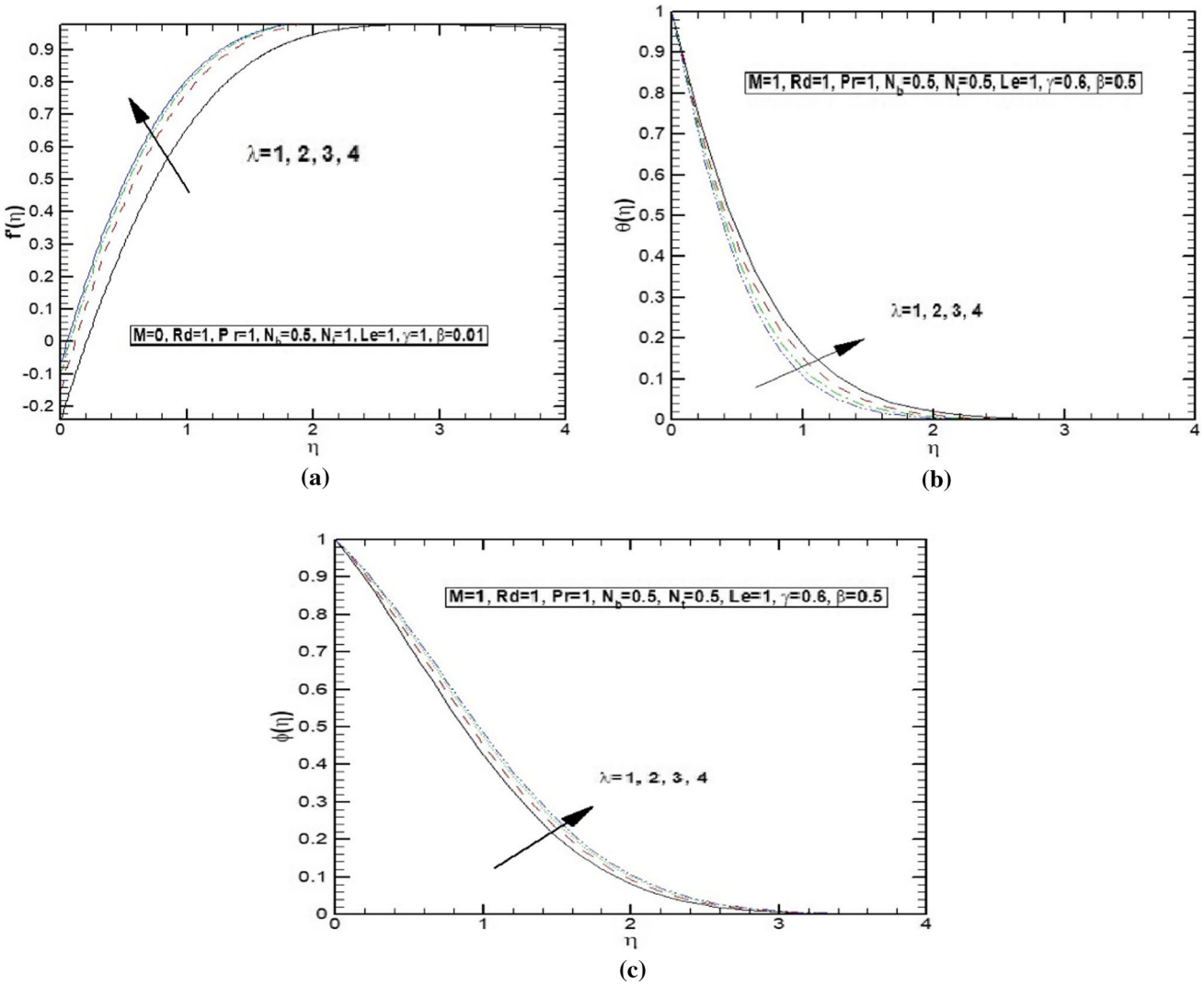


**Fig. 2** Variation of $f'(\eta)$, $\theta(\eta)$ and $\phi(\eta)$ verses $\lambda$

concentration. Figure 3a provides the influence on velocity profile $f'(\eta)$ by $\beta$. It can be noted that the slip parameter and the generalized slip parameter have the same effects.

The velocity and corresponding boundary layer thickness increasing for the higher values of the generalized slip parameter. Nevertheless, introducing the generalized slip fortifies the results for no-slip and partial slip flow. The temperature influenced by the general slip parameter for some choices of $\beta$ values is particularized in Fig. 3b. For the raising values $\beta$ of, a reduction in temperature occurred. With the introduction of lubrication on the surface, the temperature reduction becomes dominant for the higher $\beta$. A likewise behavior is executed by the concentration profile $\phi(\eta)$ sketched in Fig. 3c. However, a more conspicuous decrease is noticed for concentration species.

### 4.3 Effects of Magnetic Parameter *M*

This study considered the Lorentzian forces as well. The influence of MHD is also prominent for the temperature and concentration and the velocity of moving fluid. These impacts could be seen in Fig. 4a–c. Specifically, Fig. 4a provides the velocity evolution $f'(\eta)$ for varying magnetic parameter $M$ and by fixing the other parameters as shown in the corresponding figure. The boundary layer thickness and velocity showed the declining behavior for the growing values of the magnetic parameter.

Physically, MHD is resistive to the flow, and thus the velocity experiences a decrease with increasing values of the magnetic parameter. The higher magnetic force, the lower will be the velocity of moving fluid. A likewise

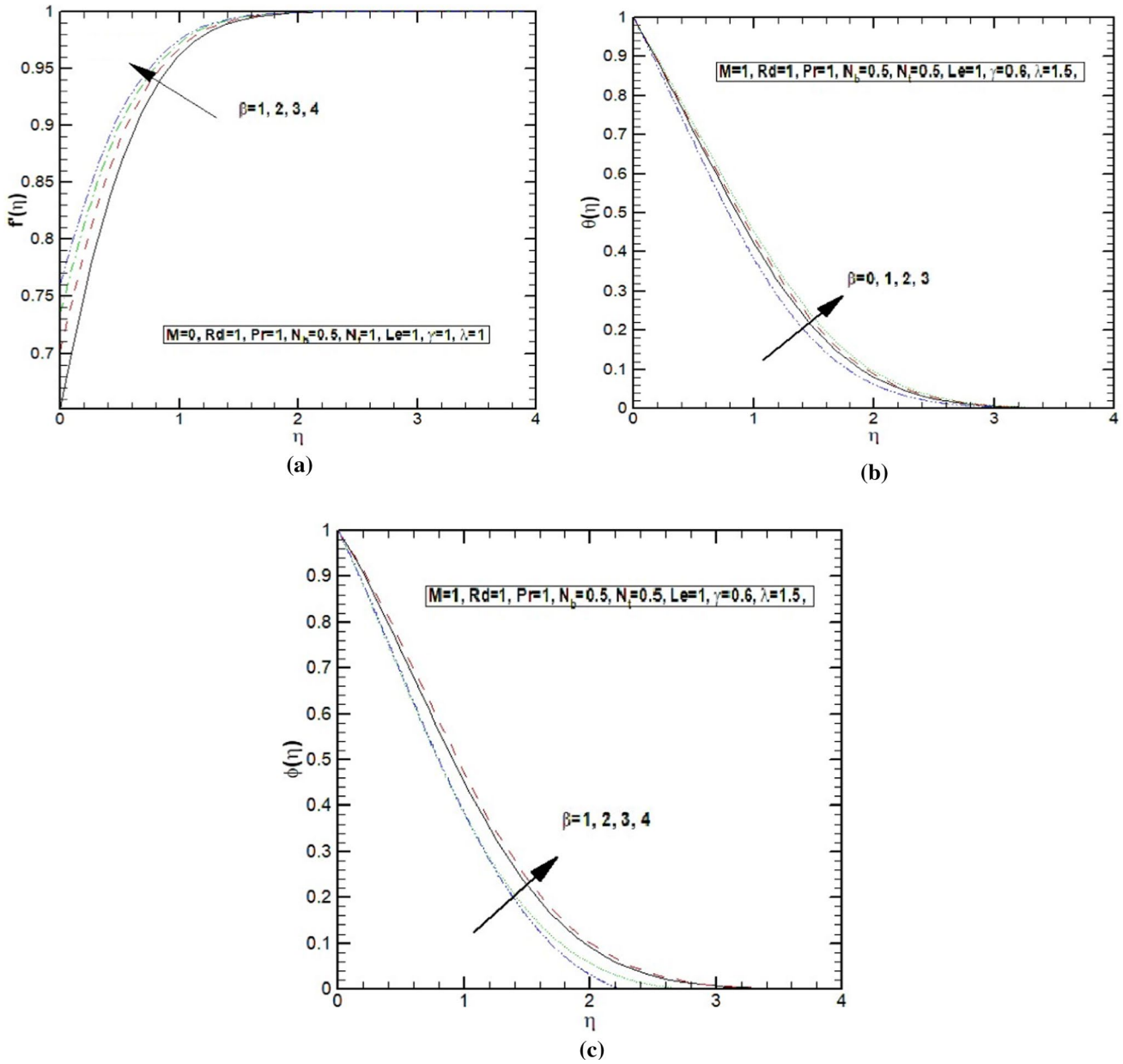


**Fig. 3** Variation of $f'(\eta)$, $\theta(\eta)$ and $\phi(\eta)$ verses $\beta$

behavior is executed by the temperature of moving fluid through the specified channel, see Fig. 4b, a reduction in the boundary layer thickness is also noticed. The concentration profile depicted in Fig. 4c executed the way as that of the temperature profile, i.e., decreasing with the increasing values of the magnetic parameter. However, we noticed the prominence of the concentration profile as compared to temperature.

### 4.4 Effects of Radiation Parameter Rd

As radiation is the source for heat transmission, so higher the radiation rate Rd the faster will be the temperature growing see Fig. 5 for the graphical illustration.

Physically, the higher rate of radiation is enhancing the surface flux that is why the increasing behavior in temperature is noticed in the boundary layer.

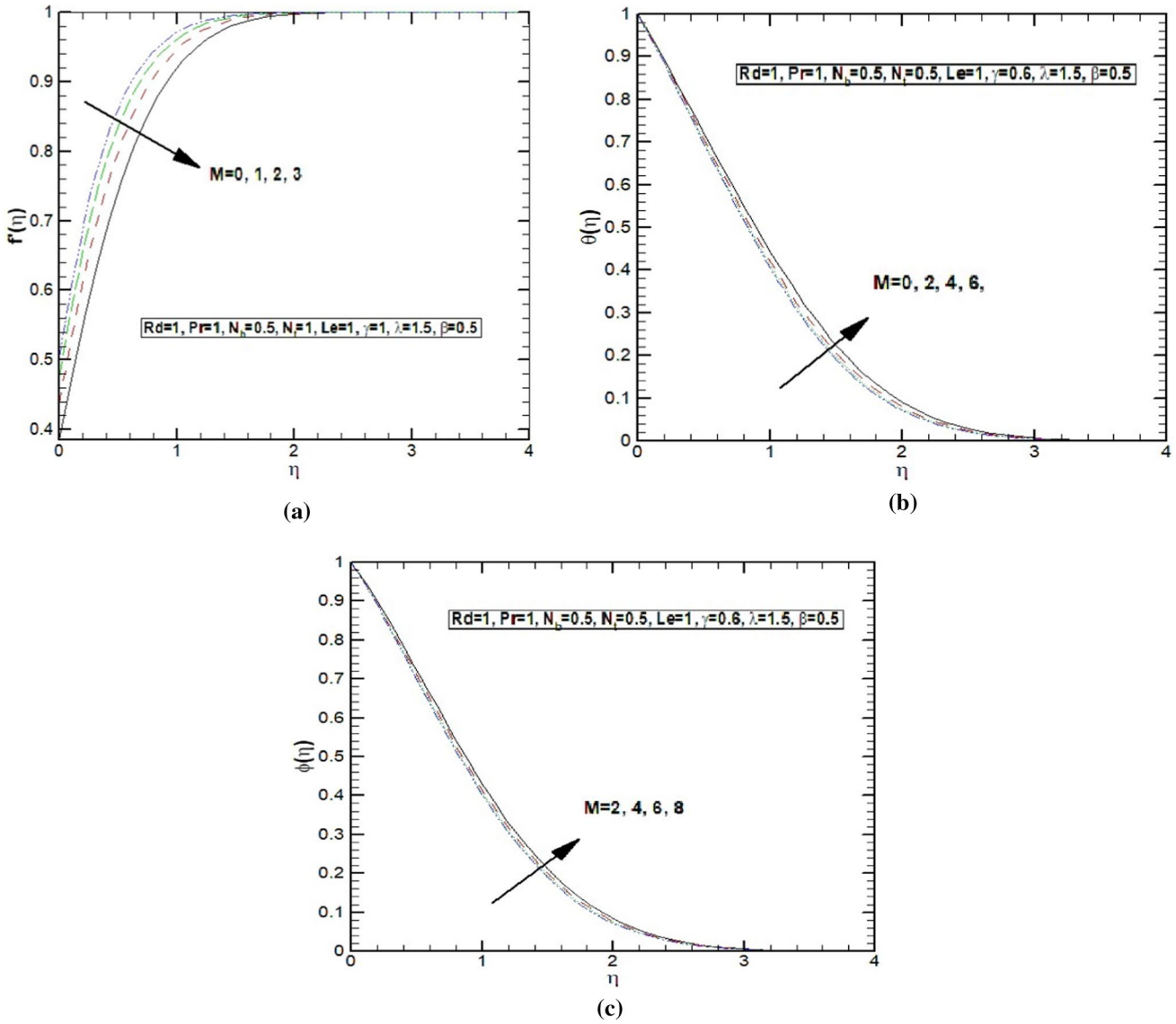


**Fig. 4** Variation of $f'(\eta)$, $\theta(\eta)$ and $\phi(\eta)$ verses $M$

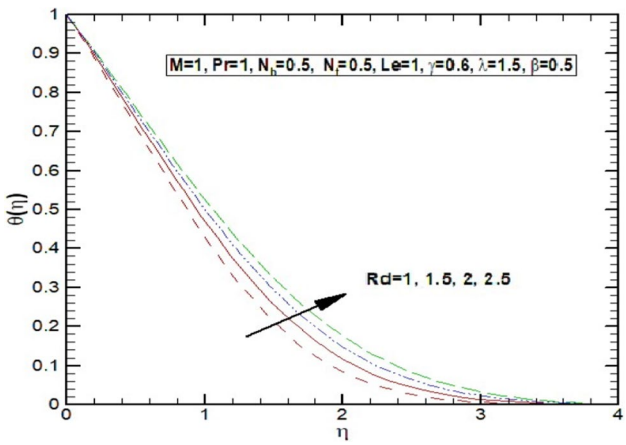


**Fig. 5** Variation of $\theta(\eta)$ verses Rd

### 4.5 Effects of Chemical Reaction Parameter $\gamma$

An increase in chemical reaction parameter $\gamma$ decreasing the concentration of the fluid, Fig. 6.

As a matter of physical fact, the concentration is significantly demolishing by chemical reaction, so that the declining behavior is shown by concentration with the growing chemical rate.

### 4.6 Effects of Thermophoresis, Brownian Motion Parameter Nb, Nt, and Le

The enhance in the temperature and concentration profiles is noticed for the growing values of these parameters. The sketch can be seen in Fig. 7a–c.

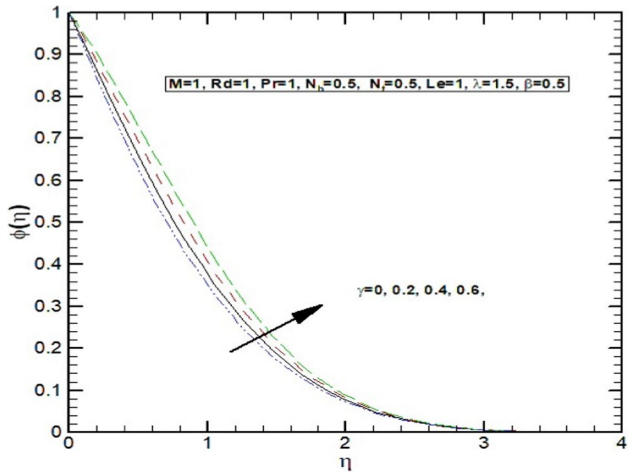


**Fig. 6** Variation of $\phi(\eta)$ verses $\gamma$

## 5 Conclusion

In this study, the Axisymmetric stagnation point flow of a magnetohydrodynamic viscous fluid over a lubricated surface with the fluid–fluid interface's generalized slip condition has been examined. A group of effecting agents is taken into account to notice velocity, temperature, and concentration by varying the involved parameters. Specifically, we considered the chemical reaction, radiation effects, the Brownian, and thermophoresis motions for their effects on the flow properties. As a result of modeling, we arrived at highly nonlinear PDEs systems, which cannot be solved by available analytic techniques. We transformed these PDEs to ODEs by applying suitable transformations preserving the fundamental laws. Finally, the ODEs are solved using BVP4C through MATLAB, which produced the numerical

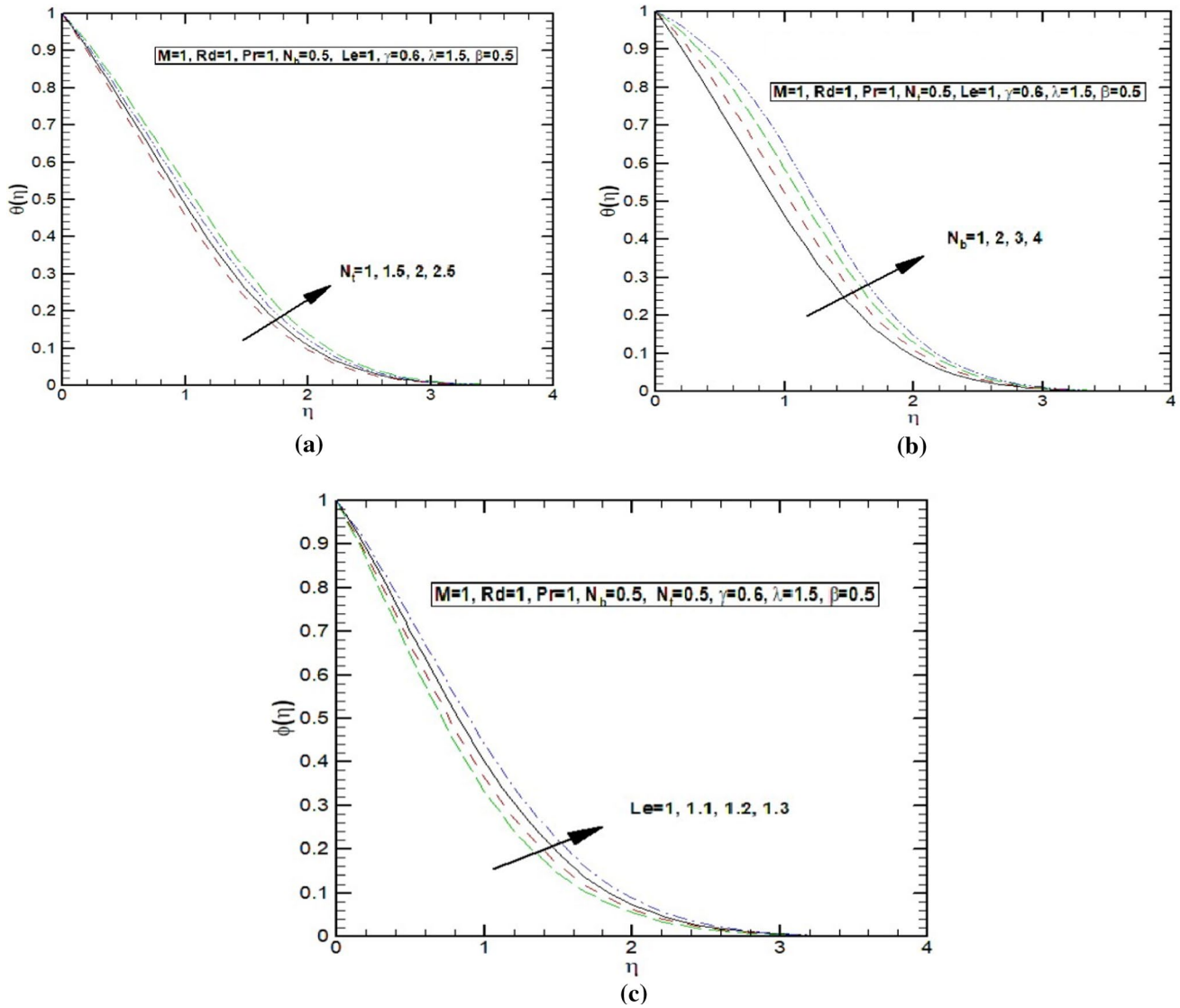


**Fig. 7** Development of **a** $\theta(\eta)$, **b** $\theta(\eta)$ and **c** $\phi(\eta)$, verses Nt, Nb, Le

**Table 1** Contrasts of the skin friction $f''(0)$ with the results in [37, 38] for $M = 0$

| $\lambda$ | Present $\beta = 0.0$ | Ref. [37] $\beta = 0.0$ | Present $\beta = 5.0$ | Ref. [38] $\beta = 5.0$ |
|---|---|---|---|---|
| 0.01 | 0.009996 | 0.009999 | 0.009902 | 0.009906 |
| 0.02 | 0.019927 | 0.019924 | 0.019561 | 0.019558 |
| 0.05 | 0.049242 | 0.049246 | 0.047082 | 0.047088 |
| 0.10 | 0.096640 | 0.096638 | 0.088783 | 0.088784 |
| 0.20 | 0.186041 | 0.186043 | 0.159723 | 0.159720 |
| 0.50 | 0.414730 | 0.414732 | 0.311099 | 0.311098 |
| 1.0 | 0.687616 | 0.687612 | 0.465619 | 0.465616 |
| 2.0 | 0.97046 | 0.97048 | 0.640374 | 0.640372 |
| 5.0 | 1.211823 | 1.211820 | 0.872404 | 0.872403 |
| 10.0 | 1.275871 | 1.275870 | 1.024092 | 1.024090 |

solutions. A comparison of the skin friction $f''(0)$ with the studies in [37, 38] is conducted in Table 1. The values of $-\theta'(0)$ (local Nusselt number) and $-\phi'(0)$ (local Sherwood number) are listed in Table 2. The vital attainments of this study are listed below:

(1) The slip parameter demolishes the impacts by the free-stream velocity
(2) It is also perceived that the Concentration losses for higher chemical reaction rate $\gamma$ and accompanied by an increased mass transfer rate.
(3) The generalized slip parameter reinforces the partial slip and no-slip conditions.
(4) With the increment of radiation parameter Rd a higher temperature distribution is recorded.

**Table 2** The values of $-\theta'(0)$ (local Nusselt number) and $-\phi'(0)$ (local Sherwood number)

| $\lambda$ | $\beta$ | $M$ | Rd | $\gamma$ | Nt | Nb | Le | Pr | $-\theta'(0)$ | $-\phi'(0)$ |
|---|---|---|---|---|---|---|---|---|---|---|
| 0.1 | 5.0 | 2.0 | 0.2 | 0.2 | 0.1 | 0.1 | 1.0 | 1.0 | 0.9516529 | 0.798065 |
| 0.5 | | | | | | | | | 0.9048014 | 0.7778584 |
| 1.0 | | | | | | | | | 0.8601858 | 0.7582466 |
| 5.0 | | | | | | | | | 0.7109313 | 0.6933064 |
| 1.0 | 0.0 | 2.0 | 0.2 | 0.2 | 0.1 | 0.1 | 1.0 | 1.0 | 0.8439852 | 0.7511538 |
| | 1.0 | | | | | | | | 0.8601858 | 0.7582466 |
| | 3.0 | | | | | | | | 0.8774733 | 0.7658315 |
| | 5.0 | | | | | | | | 1.303298 | 0.9561648 |
| 1.0 | 5.0 | 0.0 | 0.2 | 0.2 | 0.1 | 0.1 | 1.0 | 1.0 | 0.8737561 | 0.7640464 |
| | | 1.0 | | | | | | | 0.8890647 | 0.7713718 |
| | | 3.0 | | | | | | | 0.906109 | 0.7793992 |
| | | 5.0 | | | | | | | 0.9164087 | 0.7840633 |
| 1.0 | 5.0 | 2.0 | 0.1 | 0.2 | 0.1 | 0.1 | 1.0 | 1.0 | 0.932658 | 0.7539289 |
| | | | 0.5 | | | | | | 0.8170108 | 0.8284049 |
| | | | 1.0 | | | | | | 0.720456 | 0.8869271 |
| | | | 1.5 | | | | | | 0.6525194 | 0.9259482 |
| 1.0 | 5.0 | 2.0 | 0.2 | 0.1 | 0.1 | 0.1 | 1.0 | 1.0 | 0.7207534 | 0.8380918 |
| | | | | 0.5 | | | | | 0.7196422 | 1.024859 |
| | | | | 1.0 | | | | | 0.7184977 | 1.231117 |
| | | | | 1.5 | | | | | 0.717554 | 1.414464 |
| 1.0 | 5.0 | 2.0 | 0.2 | 0.2 | 0.2 | 0.1 | 1.0 | 1.0 | 1.408767 | −0.0718754 |
| | | | | | 0.3 | | | | 1.276986 | −0.3901743 |
| | | | | | 0.4 | | | | 1.357192 | −0.5271557 |
| 1.0 | 5.0 | 2.0 | 0.2 | 0.2 | 0.1 | 0.2 | 1.0 | 1.0 | 1.358604 | 0.9438171 |
| | | | | | | | | | 1.180797 | 1.098576 |
| | | | | | | | | | 1.019684 | 1.171775 |
| 1.0 | 5.0 | 2.0 | 0.2 | 0.2 | 0.1 | 0.1 | 3.0 | 1.0 | 0.7136682 | 1.756096 |
| | | | | | | | 5.0 | | 0.7114605 | 2.265156 |
| | | | | | | | 7.0 | | 0.7102361 | 2.677877 |
| 1.0 | 5.0 | 2.0 | 0.2 | 0.2 | 0.1 | 0.1 | 1.0 | 3.0 | 1.140162 | 0.7626624 |
| | | | | | | | | 5.0 | 1.382447 | 0.5902453 |
| | | | | | | | | 7.0 | 1.553301 | 0.4624992 |

(5) $-\theta'(0)$ varying directly with Pr and inversely with the other parameters. $-\phi'(0)$ varies directly with Nb, Le, and $\lambda$ on the surface.

(6) A comparison of the skin friction $f''(0)$ with the studies in [37, 38] is also conducted. A faster rate of convergence is noticed in our proposed model. See Table 1.

**Acknowledgements** The research was supported by the National Natural Science Foundation of China (Grant Nos. 11971142, 11871202, 61673169, 11701176, 11626101, 11601485). The authors extend their appreciation to the deputyship for Research & Innovation, Ministry of Education in Saudi Arabia for funding this research work through the project number (IFP-2020-10).

## References

1. Choi, S.U.S.; Eastman, J.A.: Enhancing thermal conductivity of fluids with nanoparticles. In: The Proceedings of the 1995 ASME International Mechanical Engineering Congress and Exposition, San Franciso, ASME, FED 231/MD, 66, pp. 99–105 (1995)
2. Buongiorno, J.: Convective transport in nanofluid. J. Heat Transf. **128**, 240–250 (2006)
3. Khan, W.A.; Pop, I.: Boundary layer flow of a nanofluid past a stretching sheet. Int. J. Heat Mass Transf. **53**, 2477–2483 (2010)
4. Makinde, O.D.; Aziz, A.: Boundary layer flow of a nanofluid past a stretching sheet with a convective boundary conditions. Int. J. Therm. Sci. **50**, 1326–1332 (2011)
5. Mustafa, M.; Hayat, T.; Obadait, S.: Boundary layer flow of a nanofluid over an exponentially stretching sheet with convective boundary conditions. Int. J. Numer. Methods Heat Fluid Flow **23**(6), 945–959 (2013)
6. Halim, N.A.; Noor, N.F.M.: Analytical solution for Maxwell nanofluid boundary layer flow over a stretching surface. AIP Adv. **1682**, 020006 (2015)
7. Daba, M.; Devaraj, P.: Unsteady boundary layer flow of a nanofluid over a stretching sheet with variable fluid properties in the presence of thermal radiation. Thermophys. Aerodyn. **23**(3), 403–413 (2016)
8. Ferdows, M.; Khan, M.S.; Alam, M.M.; Afify, A.A.: MHD boundary layer flow and heat transfer characteristics of a nanofluid over a stretching sheet. Acta Univ. Sapientiae Math. **9**(1), 140–161 (2017)
9. Sheikholeslami, M.: CuO-water nanofluid flow due to magnetic field inside a porous media considering Brownian motion. J. Mol. Liq. **249**, 921–929 (2018)
10. Das, K.; Sharma, R.P.; Sarkar, A.: Heat and mass transfer of a second grade magnetohydrodynamic fluid over a convectively heated stretching sheet. J. Comput. Des. Eng. **3**, 330–336 (2016)
11. Eldabe, N.T.; Moatimid, G.M.; Ali, H.S.: Magnetohydrodynamic flow of non-Newtonian visco-elastic fluid through a porous medium near an accelerated plate. Can. J. Phys. **81**(11), 1249–1269 (2003)
12. Eldabe, N.T.; Sallam, S.N.: Non-Darcy Couette flow through a porous medium of magnetohydro-dynamic visco-elastic fluid with heat and mass transfer. Can. J. Phy. **83**(12), 1243–1265 (2005)
13. Hameed, M.; Nadeem, S.: Unsteady MHD flow of a non-Newtonian fluid on a porous plate. J. Math. Anal. Appl. **325**(1), 724–733 (2007)
14. Ullah, I.; Shafie, S.; Khan, I.: Effects of slip condition and Newtonian heating on MHD flow of Casson fluid over a nonlinearly stretching sheet saturated in a porous medium. J. King Saud Univ. Sci. **29**, 250–259 (2017)
15. Shehzad, S.A.; Hayat, T.; Alsaedi, A.: Influence of convective heat and mass conditions in MHD flow of nanofluid. Bull. Pol. Acad. Sci. Tech. Sci. **63**(2), 465–474 (2015)
16. Hayat, T.; Muhammad, T.; Alsaeedi, A.; Alhuthali, M.S.: Magnetohydrodynami three-dimensional flow of viscoelastic nanofluid in the presence of nonlinear thermal radiation. J. Magn. Magn. Mater. **385**, 222–229 (2015)
17. Azimi, M.; Riazi, R.: MHD copper-water nanofluid flow and heat transfer through convergent-divergent channel. J. Mech. Sci. Technol. **30**(10), 4679–4686 (2016)
18. Azimi, M.; Riazi, R.: MHD unsteady GO-water-squeezing nanofluid flow-heat and mass transfer between two infinite parallel moving plates: analytical investigation. Sadhana **42**(3), 335–341 (2017)
19. Gireesha, B.J.; Mahanthesh, B.; Thammanna, G.T.; Sampathkumar, P.B.: Hall effects on dusty nanofluid two-phase transient flow past a stretching sheet using KVL model. J. Mol. Liq. **256**, 139–147 (2018)
20. Mahanthesh, B.; Shashikumar, N.S.; Gireesha, B.J.; Animasaun, I.L.: Effectiveness of Hall current and exponential heat source on unsteady heat transport of dusty $TiO_2$-EO nanoliquid with nonlinear radiative heat. J. Comput. Des. Eng. **6**(4), 551–561 (2019)
21. Mahanthesh, B.; Shehzad, S.A.; Ambreen, T.; Khan, S.U.: Significance of Joule heating and viscous heating on heat transport of $MoS_2$–Ag hybrid nanofluid past an isothermal wedge. J. Therm. Anal. Calorim., 1–9 (2020)
22. Kumar, P.B.; Sampath, B.; Mahanthesh, B.; Gireesha, B.J.; Shehzad, S.A.: Quadratic convective flow of radiated nano-Jeffrey liquid subject to multiple convective conditions and Cattaneo-Christov double diffusion. Appl. Math. Mech. **39**(9), 1311–1326 (2018)
23. Mahanthesh, B.; Giulio, L.; Feteh, M.O.; Isac, L.A.: Significance of exponential space-and thermal-dependent heat source effects on nanofluid flow due to radially elongated disk with Coriolis and Lorentz forces. J. Therm. Anal. Calorim., 1–8 (2019)
24. Mahanthesh, B.; Gireesha, B.J.; Gorla, R.S.R.: Unsteady three-dimensional MHD flow of a nano Eyring-Powell fluid past a convectively heated stretching sheet in the presence of thermal radiation, viscous dissipation and Joule heating. J. Assoc. Arab Univ. Basic Appl. Sci. **23**, 75–84 (2017)
25. Abbas, S.Z.; Khan, W.A.; Waqas, M.; Irfan, M.; Asghar, Z.: Exploring the features for flow of Oldroyd-B liquid film subjected to rotating disk with homogeneous/heterogeneous processes. Comput. Methods Prog. Biomed. **189**, 105323 (2020)
26. Abbas, S.Z.; Khan, W.A.; Kadry, S.; Khan, M.I.; Waqas, M.; Khan, M.I.: Entropy optimized Darcy-Forchheimer nanofluid (Silicon dioxide, Molybdenum disulfide) subject to temperature dependent viscosity. Comput. Methods Prog. Biomed. **190**, 105363 (2020)
27. Abbas, S.Z.; Khan, W.A.; Gulzar, M.M.; Hayat, T.; Waqas, M.; Asghar, Z.: Magnetic field influence in three-dimensional rotating micropolar nanoliquid with convective conditions. Comput. Methods Prog. Biomed. **189**, 105324 (2020)
28. Abbas, S.Z.; Khan, M.I.; Kadry, S.; Khan, W.A.; Israr-Ur-Rehman, M.; Waqas, M.: Fully developed entropy optimized second order velocity slip MHD nanofluid flow with activation energy. Comput. Methods Prog. Biomed. **190**, 105362 (2020)
29. Khan, W.A.; Waqas, M.; Kadry, S.; Asghar, Z.; Abbas, S.Z.; Irfan, M.: On the evaluation of stratification based entropy optimized hydromagnetic flow featuring dissipation aspect and Robin conditions. Comput. Methods Prog. Biomed. **190**, 105347 (2020)
30. Khan, W.A.; Farooq, S.; Kadry, S.; Hanif, M.; Iftikhar, F.J.; Abbas, S.Z.: Variable characteristics of viscosity and thermal conductivity in peristalsis of magneto-Carreau nanoliquid with

heat transfer irreversibilities. Comput. Methods Prog. Biomed. **190**, 105355 (2020)
31. Abbas, S.Z.; Khan, W.A.; Sun, H.; Ali, M.; Waqas, M.; Irfan, M.; Ahmad, S.: Modeling and analysis of von Kármán swirling flow for Oldroyd-B nanofluid featuring chemical processes. J. Braz. Soc. Mech. Sci. Eng. **41**(12), 556 (2019)
32. Abbas, S.Z.; Shah, H.H.; Sun, H.; Rahaman, F.; Ahmed, F.: Gravitational collapse of dust fluid and dark energy in the presence of curvature: black hole formation. Mod. Phys. Lett. A **34**(29), 1950240 (2019)
33. Hayat, T.; Khan, W.A.; Abbas, S.Z.; Nadeem, S.; Ahmad, S.: Impact of induced magnetic field on second-grade nanofluid flow past a convectively heated stretching sheet. Appl. Nanosci. **10**, 3001–3009 (2020). https://doi.org/10.1007/s13204-019-01215-x
34. Abbas, S.Z.; Khan, W.A.; Sun, H.; Irfan, M.; Khan, M.I.; Waqas, M.: Von Kármán swirling analysis for modeling Oldroyd-B nanofluid considering cubic autocatalysis. Phys. Scr. **95**(1), 015206 (2019)
35. Abbas, S.Z.; Khan, W.A.; Sun, H.; Ali, M.; Irfan, M.; Shahzed, M.; Sultan, F.: Mathematical modeling and analysis of Cross nanofluid flow subjected to entropy generation. Appl. Nanosci. **10**(8), 3149–3160 (2020)
36. Ali, W.; Mahmood, S.; Chammam, W.; Ul-Haq, W.; Khan, W.A.; Abbas, S.Z.: Mathematical modeling and chemical conduct considering non-Newtonian nanofluid by utilizing heat flux features. Soft Comput., 1–11 (2020)
37. Santra, B.; Dandapat, B.S.; Andersson, H.I.: Axisymmetric stagnation-point flow over a lubricated surface. Acta Mech. **194**, 1–10 (2007)
38. Sajid, M.; Mahmood, K.; Abbas, Z.: Axisymmetric stagnation-point flow with a general slip boundary condition over a lubricated surface. Chin. Phys. Lett. **29**, 024702 (2012)